Fabrication, Structural Characterization and Testing of a Nanostructured Tin Oxide Gas Sensor

James G. Partridge, Matthew R. Field, Abu Z. Sadek, *Student Member, IEEE*, Kourosh Kalantar-zadeh, Johan Du Plessis, Matthew B. Taylor, Armand Atanacio, Kathryn E. Prince, and Dougal G. McCulloch

***Abstract*—A nanostructured SnO_2 conductometric gas sensor was produced from thermally evaporated Sn clusters using a thermal oxidation process. SnO_2 clusters were simultaneously formed in an identical process on a Si_3N_4 membrane featuring an aperture created by a Focused Ion Beam (FIB). Clusters attached to the vertical edges of the aperture were imaged using a transmission electron microscope. The original morphology of the Sn cluster film was largely preserved after the thermal oxidation process and the thermally oxidized clusters were found to be polycrystalline and rutile in structure. NO_2 gas sensing measurements were performed with the sensor operating at various temperatures between 25°C and 290 °C. At an operating temperature of 210 °C, the sensor demonstrated a normalized change in resistance of 3.1 upon exposure to 510 ppb of NO_2 gas. The minimum response and recovery times for this exposure were 45 s and 30 s at an operating temperature of 265 °C. The performance of the SnO_2 sensor compared favorably with previously published results. Finally, secondary ion mass spectrometry and X-ray photoelectron spectroscopy were used to establish the levels of nitrogen present in the films following exposure to NO_2 gas.**

***Index Terms*—Gas detectors, microscopy, nanotechnology, thin-film devices.**

I. Introduction

RUTILE tin oxide (SnO_2) is a wide band-gap n-type semiconductor which has been employed as a gas sensing material for many years [1]. Adsorption of oxidants or reducing agents on the SnO_2 surface causes a change in the depth of the electron-depletion layer below the surface and a corresponding change in the resistance of the material. For example, if a film of SnO_2 at a temperature between 100 °C and 500 °C is exposed to NO_2 gas, ionosorption of oxygen (in its molecular and atomic forms) occurs and the depletion layer width increases [2], [3]. This produces a concentration dependent increase in resistance and thereby provides the sensing mechanism. A change in the operating temperature of a SnO_2 sensor produces changes in the rates of the surface adsorption and desorption processes and a change in the energy required to activate them. Consequently, the sensitivity of SnO_2 to oxidizing and reducing gases is temperature dependent [3]. Nanostructured SnO_2 sensors have been produced by various research groups, as their surface-to-volume ratio is large and the gas-surface interaction can take place on both sides of a grain or neck instead of only on the top surface, as in the case of a compact film [2]. With careful process control, feature sizes can be made comparable to the depth of the depletion layer. This can yield very high sensitivity since pathways through the conducting network can become completely "pinched-off" above a certain exposure level. The effects of the feature (grain) size have been studied in detail by various authors (see, for example, [2]–[4]). Despite the growing number of techniques for producing nanostructured SnO_2 sensors, it is widely acknowledged that the relationship between the electrical and nanostructural properties of SnO_2 gas sensing films is not yet fully understood [2].

Physical vapor deposition methods used to produce SnO_2 films include pulsed laser deposition [5], sputtering [6], and evaporation [7]. It is also possible to deposit Sn films in an inert atmosphere, and subsequently transform them into SnO_2 using a thermal annealing process. The rheotaxial growth and thermal oxidation (RGTO) process [7], [8] is commonly used to transform porous Sn thin-films into SnO_2 as the morphology of the original film is substantially retained after the transformation. The technique has also been employed to produce SnO_2 nanowires from Sn nanowires [9]. In this method, the Sn sample is heated in the presence of oxygen to a temperature just below the Sn melting point to promote growth of a native oxide shell. The oxide shell retains its shape during a high-temperature oxidation process (typically, 600 °C–700 °C) which follows and thus the morphology/dimensions of the film/nanowire can be preserved. Using cross-sectional transmission electron microscopy (TEM), we recently confirmed that the morphology of the Sn cluster film remained largely unaltered after the RGTO process [10] and that full conversion to SnO_2 was achieved using a 600 °C oxidation temperature.

In this work, we have fabricated a nanostructured RGTO processed SnO_2 sensor and determined its sensitivity to NO_2 gas over an operating temperature range of 25 °C to 290 °C. A novel sample preparation method enabled TEM imaging of the SnO_2 film before and after oxidation. High-resolution images of the interior of SnO_2 clusters were obtained without sectioning samples using this technique. Secondary ion mass spectrometry and X-ray photoelectron spectroscopy were then used to measure the nitrogen content in the films.

Manuscript received October 15, 2008; accepted November 14, 2008. Current version published April 10, 2009. This work was supported in part by the Australian Research Council and in part by the Australian Institute of Nuclear Science and Engineering under Grant 331978. The associate editor coordinating the review of this paper and approving it for publication was Prof. Evgeny Katz.

J. G. Partridge, M. R. Field, J. Du Plessis, M. B. Taylor, and D. G. McCulloch are with the School of Applied Sciences, Royal Melbourne Institute of Technology, Melbourne, VIC 3001, Australia (e-mail: jim.partridge@rmit.edu.au).

A. Sadek and K. Kalantar-zadeh are with the School of Electronic and Computer Engineering, Royal Melbourne Institute of Technology, Melbourne, VIC 3001, Australia.

A. Atanacio and K. E. Prince are with the Australian Nuclear Science and Technology Organization, Menai, New South Wales 2234, Australia.

Digital Object Identifier 10.1109/JSEN.2009.2016613

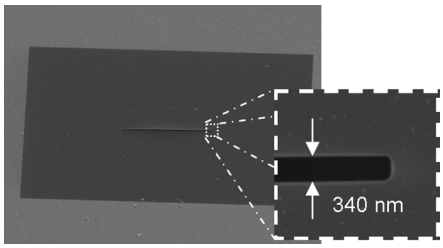

Fig. 1. A Si_3N_4 membrane with an aperture-slot etched using a focused ion beam.

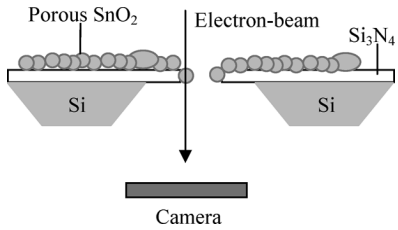

Fig. 2. Schematic diagram showing a SnO_2 cluster coated Si_3N_4 membrane with Sn and SnO_2 clusters attached to the walls of the etched slot and the electron-beam used to image them.

II. Experiment

A. Sample Preparation

The SnO_2 films were deposited on P-type Si substrates with a 1-μm-thick layer of SiO_2 separating the SnO_2 layer from the Si substrate. Planar electrical contacts on the sensor were fabricated using a photo-plot mask and optical lithography. The total length of each interdigital-type contact was approximately 35 mm and the contact-to-contact separation was approximately 100 μm.

The Si_3N_4 membranes (designed to fit into a standard TEM sample holder) were purchased from SPI Supplies [11]. Slots with $\sim$ 330 nm width and 25 μm length were etched through the 50 nm thick membranes (as shown in Fig. 1) using a FEI Nova Focused Ion Beam system with an ion beam dose of 0.1 $nC/\mu m^2$ at 0.2 pA beam current.

B. Deposition of Sn and Thermal Oxidation to Form SnO_2

The membrane and contacted substrate were mounted in the deposition chamber of a Dynavac thermal evaporator. In order to ensure that the samples experienced identical deposition conditions, they were situated in close proximity to each other. The deposition rate was 0.2 ± 0.05 nm/s (measured using a quartz crystal film thickness monitor) and the base pressure and process pressure were 1×10^{-6} Torr and 5×10^{-6} Torr, respectively. After depositing a Sn layer of nominal thickness 80 nm, the coated sensor substrate and Si_3N_4 membrane were heated in air at atmospheric pressure using a simple bench-top furnace. The temperature sequence for the thermal oxidation was 200 °C (2 h), then 400 °C (2 h) and, finally, 600 °C (2 h) with 30-min ramp times between each temperature. Once complete, the SnO_2 coated sensor substrate was placed in a multichannel gas calibration system. The contact-to-contact resistance was then measured in synthetic air and during timed exposures to various concentrations of NO_2 gas (provided from a bottle consisting of 8.5 ppm NO_2 in dry synthetic air).

C. Microscopy and X-Ray Photoelectron Spectroscopy

A JEOL 2010 TEM operating at 200 kV was used to provide images of the nanostructure within the clusters. Fig. 2 shows schematically how the Sn coated Si_3N_4 membrane samples were positioned in the TEM and how images of clusters on the vertical walls of the etched slot were obtained. X-ray photoelectron spectroscopy (XPS) was also performed on the Sn and SnO_2 cluster films using a VG Microlab 310 F with a 1486.6 eV Al anode X-ray source operated at a power of 300 W and with a 15 kV excitation voltage. The samples were tilted such that the electron analyzer was normal to the sample surface. The analyzed rectangular area was approximately 5×1 mm^2. All samples were sputtered *in situ* with Ar ions in order to remove carbon contaminants from the surface. A SnO_2 powder standard [12] was used to calibrate the sensitivity factors prior to the measurements. The scan was centered over the C1s, Sn3d, and O1s binding energy peaks with a pass energy of 20 eV and an energy step size of 0.1 eV. A Sn3d5 sensitivity factor of 21.00 was determined to be correct.

Depth profiling of the nitrogen levels within the samples was performed by sputtering away the sample *in situ* using a 3 kV Ar sputtering beam. A broad spectrum scan was acquired using a pass energy of 50 eV and energy step size of 0.1 eV. The areas under the N1s and C1s peaks were fitted, and sensitivity factors from the Scofield (Al Source) library [13] were applied to determine the relative atomic percentages of nitrogen and carbon through the depth of the samples.

D. Secondary Ion Mass Spectroscopy (SIMS)

A Cameca 5 f Dynamic Secondary Ion Mass Spectrometer (SIMS) was used to determine the composition of the SnO_2 films. Specifically, a depth profile of the nitrogen content was measured for three films prepared under identical conditions but having different exposures to NO_2 gas. Cs^+ ions were used to probe the sample at normal incidence and the primary accelerating voltage was 2.4 kV. The beam diameter was 20 μm and the analyzed area was approximately 250×250 μm^2. The total acquisition time per sample was approximately 800 s.

E. Gas Sensing Measurements

The sensor was mounted on an alumina microheater in the test multichannal gas chamber. The microheater was controlled by a regulated DC power supply and provided operating temperatures up to 300 °C. A gas calibration system, with computer interfaced mass flow controllers, was used to expose the sensor to different concentrations of NO_2 gas. The sensor resistance was measured continuously using a multimeter (Keithley 2001) that was also interfaced with a personal computer. The total flow rate was kept constant at 200 sccm and since SnO_2 is sensitive to humidity [14], synthetic air (certified zero humidity) was used as the reference gas.

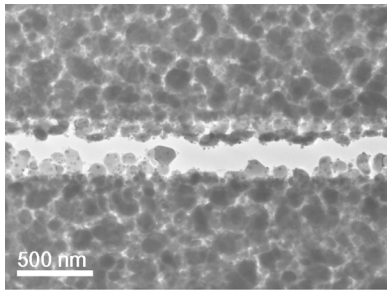

(a)

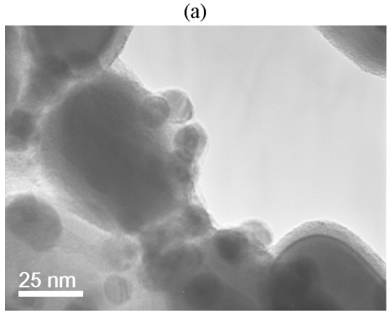

(b)

Fig. 3. The as-deposited Sn clusters attached to the Si_3N_4 membrane and imaged at (a) low-magnification and (b) higher magnification.

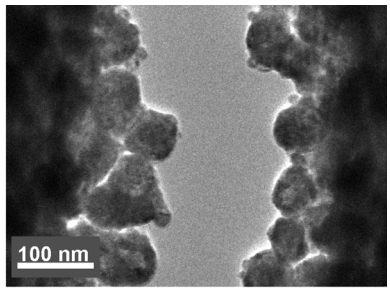

(a)

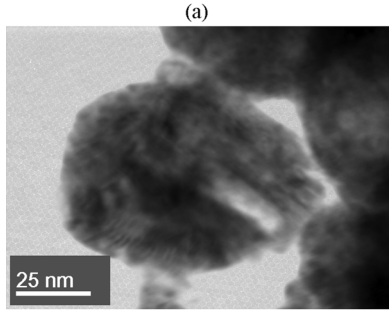

(b)

Fig. 4. The oxidized Sn clusters attached to the Si_3N_4 membrane and imaged at (a) low-magnification and (b) higher magnification.

III. Results and Discussion

A. *TEM Characterization of* SnO_2 *on* Si_3N_4 *Membranes*

Fig. 3 shows a Sn cluster film supported on a Si_3N_4 membrane and imaged immediately after the deposition process. Significant coalescence between neighboring clusters caused the Sn films on the sensor and Si_3N_4 membrane to appear coral-like in morphology, however, discrete clusters could still be found under the TEM. The average cross-sectional area of these clusters was measured using image processing software and found to be approximately 1×10^4 nm^2. As shown in Fig. 3(b), the as-deposited Sn films contained irregular shaped clusters with thin surface oxide shells surrounding the Sn cores. The majority of the oxide layer would have grown after the Si_3N_4 membrane was removed from the vacuum deposition system.

Following oxidation at 600 °C, the discrete cores and oxide shells were no longer visible and the nanostructure of the SnO_x clusters became more complex, containing small voids and crystallites (Fig. 4). The crystallites observed in the oxidised clusters had cross-sectional areas of between 5 nm^2 and 500 nm^2. Selected area diffraction patterns from the as-deposited and oxidized Si_3N_4 membrane samples (not shown) could be indexed to metallic Sn and rutile SnO_2, respectively. The TEM images and diffraction patterns showed no preferred orientation of the SnO_2 and no evidence could be found for metallic Sn reflections in the diffraction pattern from the oxidized sample, indicating that the Sn clusters had fully transformed into SnO_2 after the oxidation process. This assertion was supported using XPS which showed that Sn, SnO and SnO_2 were present in the as-deposited sample but only SnO_2 was present after oxidation [10].

Fig. 5 shows the same area of the membrane/film before [Fig. 5(a)] and after [Fig. 5(b)] thermal oxidation. In Fig. 5(a), the clusters consist of Sn cores with oxide shells (as in Fig. 3), while in Fig. 5(b), the clusters consist of polycrystalline SnO_2 but largely retain their original shape. Unlike conventional TEM samples, the Si_3N_4 membrane can be fabricated quickly and the sensing film can be imaged immediately after each process without exposure to epoxy or other chemicals. Importantly, the Si_3N_4 membrane withstood the FIB etching, the thermal oxidation process and numerous transfers between microscopes and deposition systems. Inspection of thermally treated nanoparticles/nanowires composed from other materials should therefore be possible using this method.

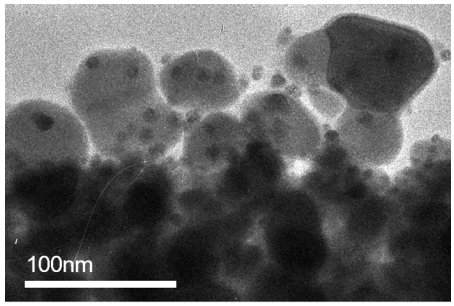

(a)

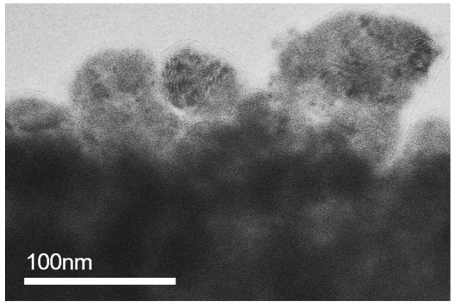

(b)

Fig. 5. (a) Nonoxidized and (b) oxidized Sn clusters attached to the Si_3N_4 membrane. These images show the same location on the Si_3N_4 membrane.

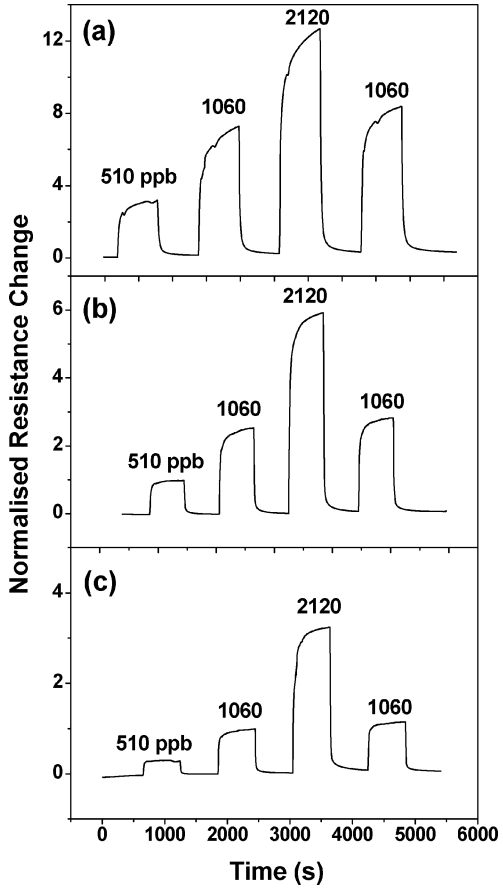

Fig. 6. The normalized change in resistance ($\Delta R/R_0$) exhibited by the nanostructured SnO_2 film when exposed to different concentrations of NO_2 and operated at: (a) 210 °C; (b) 265 °C; and (c) 290 °C. (R_0 is the resistance at the selected operating temperature in synthetic air, R is the maximum resistance reached at the selected operating temperature for a given concentration of NO_2 gas and $\Delta R = R - R_0$).

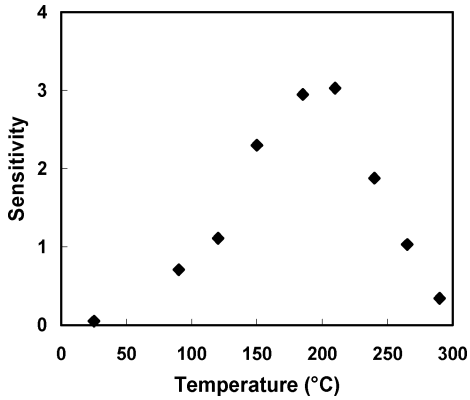

Fig. 7. The maximum normalized change in resistance ($\Delta R/R_0$) measured with a NO_2 gas concentration of 510 ppb for various operating temperatures.

B. Gas Sensing Measurements

The normalized change in the resistance of the SnO_2 gas sensor during exposure to various concentrations of NO_2 and at three different operating temperatures is shown in Fig. 6. The sequence of NO_2 concentrations inlet to the sample chamber was 510 ppb, 1.06 ppm, 2.12 ppm, and a repeat 1.06 ppm. Each concentration was inlet as a pulse in between periods in which synthetic air was inlet to the chamber. The difference in the baseline resistance (with no NO_2 gas present) before and after each sequence of NO_2 pulses was less than 5% in the temperature range 150 °C–290 °C and the reproducibility in response was within 15% in the same temperature range. A film exposed for 36 h to 2120 ppb of NO_2 at 265 °C did, however, exhibit a significant permanent increase in its baseline resistance (in synthetic air) from 4.6 kΩ (before exposure) to 5.2 kΩ (after exposure).

The maximum measured sensitivity was observed at a temperature of 210 °C (see Fig. 7), while the minimum response and recovery times occurred when the sensor was operated at 265 °C. With an NO_2 concentration of 510 ppb, these times were 45 s and 30 s, respectively, at 265 °C, and 180 s and 130 s, respectively, at 210 °C.

These results are consistent with previously observed sensing behavior in porous SnO_2 films which exhibit an asymmetric bell-shaped variation of the gas sensitivity with the sensor operation temperature [15]. The temperature at which the maximum sensitivity occurs is also dependant on the concentration of the gas [15]. The resistance changes observed in the sensor are due to the temperature dependant chemisorption of NO_2 at the surface of the SnO_2. If electronegative NO_2 molecules approach the surface of the SnO_2 with electron affinities greater than the semiconductor work function, the molecules will each pick up an electron from the SnO_2 conduction band and become chemisorbed at the surface. The width of the electron depletion layer and the height of potential barrier that surround the SnO_2 clusters both increase as a result of the increased surface charge [16].

The thickness of the depletion region within the clusters is reduced at high-temperatures due to an increase in thermal ionization, and hence carrier concentration [17]. As a result, the proportional change in the thickness of the nondepleted region (within each cluster/neck) may be lower at higher temperatures, contributing to a smaller change in the normalized resistance. The response and recovery times decrease with increasing temperature because the thermally activated adsorption and desorption processes occur (and balance out to equilibrium) more rapidly [17] and because the penetration of the gas into the sensing layer decreases [15].

C. SIMS and XPS Measurements

SIMS was used to measure the relative amounts of nitrogen in a "high-exposure" sample ($\sim$ 36-h with 2120 ppb NO_2 at 265 °C), a "low-exposure" sample (12 h with 2120 ppb NO_2 at 265 °C), and a nonexposed, nonheated SnO_2 cluster film. The results are shown in Fig. 8. In the SIMS process, approximately 100 s of etching was required to remove surface contaminants (expected to be predominantly carbon) from the porous tin oxide layer. The measurements taken after this period clearly show that increased exposure time led to increased retention of nitrogen in the SnO_2 cluster films. This may have contributed to the $\sim$ 5% change in the baseline resistance observed in the "high-exposure" sample. In order to quantify the nitrogen trace derived from SIMS, XPS depth profiling was performed. Fig. 9(a) shows a XPS depth profile from the nonexposed, non-heated SnO_2 film and Fig. 9(b) shows a XPS profile from the "low-exposure" (12 h with 2120 ppb NO_2 at 265 °C) SnO_2

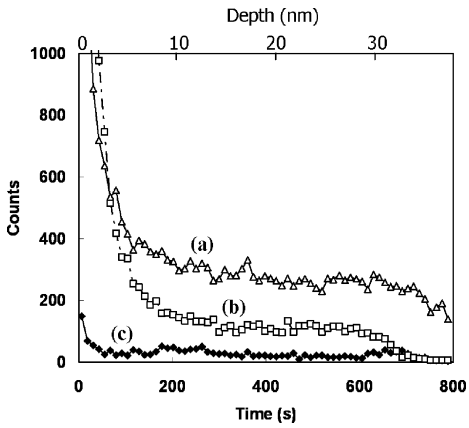

Fig. 8. SIMS counts versus time for three nanostructured SnO_2 films after gas exposures of: (a) 2120 ppb NO_2 at 265 °C for 36 h; (b) 2120 ppb NO_2 at 265 °C for 12 h; and (c) no exposure, no heating (as-deposited).

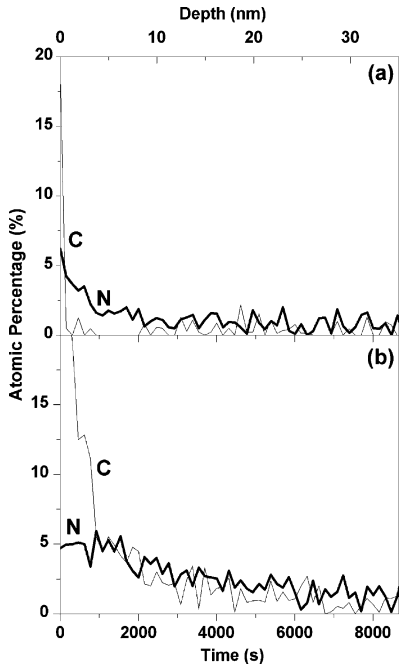

Fig. 9. XPS depth profile of (a) unexposed and (b) exposed SnO_2 films showing the concentration of nitrogen and carbon.

film. As in the SIMS measurements, a significant contamination level existed at the surface so the nitrogen levels were measured after this contamination layer was removed. The average level of nitrogen in the subsurface of the low-exposure sample was found to be 1.8%, compared to 0.85% for the unexposed sample. Using this data as a basic calibration suggests that the nitrogen level in the sensor was greater than 3%.

IV. Conclusion

The RGTO technique was used to prepare SnO_2 clusters from discontinuous evaporated Sn thin films on a conductometric sensor substrate and a Si_3N_4 membrane featuring an aperture-slot. The temperature dependent response of the SnO_2 conductometric gas sensor was measured for various concentrations of NO_2 gas. Transmission electron microscopy of Sn and SnO_2 clusters adhered to the walls of the aperture-slot was performed before and after the thermal oxidation process. Selected area diffraction analysis showed that after oxidation at 600 °C, the clusters were transformed to polycrystalline rutile SnO_2. The estimated volumetric change of the clusters after oxidation was $\sim 50\%$ but the morphology of the cluster films was largely preserved after the RGTO process. The slotted membrane method provided similar information to cross-sectional TEM but with greatly reduced sample preparation time. This method could also be employed to inspect clusters made from a wide variety of materials and deposited using a variety of physical vapor deposition or wet-chemical techniques. The significant retention of nitrogen found using SIMS and XPS may be a contributing factor in the "ageing" effects (changing baseline resistance) commonly observed in nanoporous SnO_2 sensors and warrants further investigation.

Acknowledgment

The authors would like to thank S. Rubanov for assistance with FIB etching.

References

[1] K. Ihokura and J. Watson, *The Stannic Oxide Gas Sensor: Principles and Applications*. Boca Raton, FL: CRC Press, 1994.
[2] N. Barsan, M. Schweizer-Berberich, and W. Göpel, "Fundamental and practical aspects in the design of nanoscaled SnO_2 gas sensors: A status report," *J. Anal. Chem.*, vol. 365, no. 4, pp. 287–304, Oct. 1999.
[3] N. Barsan and U. Weimar, "Conduction model of metal oxide gas sensors," *J. Electroceramics*, vol. 7, no. 3, pp. 143–167, Dec. 2001.
[4] T. P. Hülser, H. Wiggers, F. E. Kruis, and A. Lorke, "Nanostructured gas sensors and electrical characterization of deposited SnO_2 nanoparticles in ambient gas atmosphere," *Sens. Actuators B*, vol. 109, no. 1, pp. 13–18, Aug. 2005.
[5] M. A. El Khakani, R. Dolbec, A. M. Serventi, M. C. Horrillo, M. Trudeau, R. G. Saint-Jacques, D. G. Rickerby, and I. Sayago, "Pulsed laser deposition of nanostructured tin oxide films for gas sensing applications," *Sens. Actuators B*, vol. 77, no. 1, pp. 383–388, Jun. 2001.
[6] G. Micocci, A. Tepore, A. Serra, P. Siciliano, and Z. Ali-Adib, "CO sensing characteristics of reactively sputtered SnO_2 thin films prepared under different oxygen partial pressure values," *Vacuum*, vol. 47, no. 10, pp. 1175–1177, Oct. 1996.
[7] G. Sberveglieri, G. Faglia, S. Groppelli, P. Nelli, and A. Camanzi, "A new technique for growing large surface area SnO_2 thin film (RGTO technique)," *Semicond. Sci. Technol.*, vol. 5, no. 12, pp. 1231–1233, Dec. 1990.
[8] X. Q. Pan and L. Fu, "Oxidation and phase transitions of epitaxial tin oxide thin films on (1012) sapphire," *J. Appl. Phys.*, vol. 89, no. 11, pp. 6048–6055, Jun. 2001.
[9] A. Kolmakov, Y. Zhang, and M. Moskovits, "Topotactic thermal oxidation of Sn nanowires: Intermediate suboxides and core-shell metastable structures," *Nano Lett.*, vol. 3, no. 8, pp. 1125–1129, Jul. 2003.
[10] J. G. Partridge, M. Field, J. L. Peng, A. Z. Sadek, K. Kalantar-zadeh, J. Du Plessis, and D. G. McCulloch, "Nanostructured SnO_2 films prepared from evaporated Sn and their application as gas sensors," *Nanotechnology*, vol. 19, no. 12, p. 125504 (5pp), Mar. 2008.
[11] SPI Supplies, Prod. No. 4096SN-BA.
[12] Sigma Aldrich SnO_2 99.9%–325 Mesh, Prod. No. 244651-100G.
[13] J. H. Scofield, "Hartree-Slater subshell photoionization cross-sections at 1254 and 1487 eV," *J. Electron Spectrosc. Relat. Phenom.*, vol. 8, pp. 129–137, 1976.
[14] J. Santos, P. Serrini, B. O'Beirn, and L. Manes, "A thin film SnO_2 gas sensor selective to ultra-low NO_2 concentrations in air," *Sens. Actuators B, Chem.*, vol. 43, no. 1, pp. 154–160, Sep. 1997.
[15] S. Ahlers, G. Müller, and T. Doll, "A rate equation approach to the gas sensitivity of thin film metal oxide materials," *Sens. Actuators B, Chem.*, vol. 107, no. 2, pp. 587–599, Jun. 2005.
[16] S.-C. Chang, "Thin-film semiconductor NO_x sensor," *IEEE Trans. on Electron Devices*, vol. 26, no. 12, pp. 1875–1880, Dec. 1979.
[17] P. T. Moseley and A. J. Crocker, *Sensor Materials*. Bristol, U.K.: Institute of Physics Publishing, 1996, pp. 71–74.

Jim G. Partridge received the B.Sc. and Ph.D. degrees in physics from the University of Bath, Bath, U.K., in 1996 and 2000, respectively.

His research interests include nanofabrication, microscopy, and chemical sensors. He is a Research Fellow at the School of Applied Sciences at the Royal Melbourne Institute of Technology, Melbourne, Australia.

Matthew R. Field received the B.Sc. (Hons) degree in applied physics from the Royal Melbourne Institute of Technology (RMIT), Melbourne, Australia, in 2005 and 2006, respectively. He is currently working towards the Ph.D. degree at the School of Applied Sciences, RMIT University.

He specializes in the micro-analysis of metal oxide thin films.

Abu Z. Sadek (S'06) received the M.E. degree in telecommunications engineering from the University of Melbourne, Melbourne, Australia, in 2002 and the Ph.D. degree in electronics and communications engineering from the Royal Melbourne Institute of Technology (RMIT), Melbourne, Australia, in 2008.

He is a Postdoctoral Fellow in the School of Electrical and Computer Engineering, RMIT University. His research interests include chemical sensors, solar cells, nanotechnology, and conducting polymers.

Kourosh Kalantar-zadeh received the B.Sc. and M.Sc. degrees from the Sharif University of Technology, Tehran, Iran, and Tehran University, Tehran, and the Ph.D. degree from the Royal Melbourne Institute of Technology (RMIT), Melbourne, Australia.

He is now a Senior Lecturer at the School of Electrical and Computer Engineering, RMIT University. His research interests include chemical and biochemical sensors, nanotechnology, microsystems, materials science, electronic circuits, and microfluidics.

Johan Du Plessis received the B.Sc. (Hons) degree in physics and the Ph.D. degree from the University of the Free State, Bloemfontein, South Africa, in 1977 and 1987, respectively.

He is currently at the School of Applied Sciences at the Royal Melbourne Institute of Technology (RMIT), Melbourne, Australia, and his research focuses on the characterization of surfaces and thin films using surface analytical techniques.

Matthew B. Taylor received the B.Sc. and Ph.D. degrees in physics from the Royal Melbourne Institute of Technology (RMIT), Melbourne, Australia, in 1999 and 2003, respectively.

He is a Postdoctoral Research Scientist in the School of Applied Sciences at RMIT University. His research interests include thin-film deposition and electron microscopy techniques.

Armand Atanacio is currently working towards the Ph.D. degree at the Centre for Materials Research in Energy Conversion, University of New South Wales, NSW, Australia.

He specializes in surface analysis of materials using secondary ion mass spectrometry. He is a Scientist in the Beam Technologies Program at the Australian Nuclear Science and Technology Organization, Menai, New South Wales, Australia.

Kathryn E. Prince received the B.Sc. (Hons) and Ph.D. degrees in geology.

She has research expertise in SIMS, SEM, and other microbeam and radioisotopic techniques. She is an Adjunct Associate Professor in the School of Materials Science and Engineering, University of New South Wales, and manages the SIMS facility at ANSTO.

Dougal G. McCulloch received the B.Sc. and Ph.D. degrees in physics from the Royal Melbourne Institute of Technology (RMIT), Melbourne, Australia, in 1988 and 1994, respectively.

His research interests include carbonaceous solids, thin-film coating materials, transmission electron microscopy, and electron energy loss spectroscopy. He is the Director of the Microscopy and Microanalysis Facility, RMIT University.